

---

---

# Capillary morphogenesis during healing of full-thickness skin grafts: An ultrastructural study

**MICHAEL J. GORETSKY, MD; MATTHEW BREEDEN, BS; GREGORY PISARSKI, MD; M. DANA HARRIGER, PhD; STEVEN T. BOYCE, PhD; DAVID G. GREENHALGH, MD, FACS**

---

Biologic mechanisms by which skin grafts become revascularized after transplantation are poorly understood. To investigate graft revascularization, we examined the pattern of capillary growth in full-thickness skin grafts at serial time points. Full-thickness skin (2 x 2 cm) was excised to muscle fascia from the bilateral hind limbs of adult male Lewis rats. The graft/wound base boundary was identified by placement of a polypropylene mesh on the wound beneath the graft. Excised skin was replaced in its original orientation and secured with silk sutures tied over a gauze bolster dressing. After 3, 5, 7, and 10 days, animals were killed, and their aortas were cannulated and infused with an acrylic polymer to generate vascular casts. Grafts were excised, tissues were digested, and casts were examined with the use of scanning electron microscopy. Transmission electron microscopy was performed on tissues infused with the acrylic polymer that were not digested. At day 3, an immature lobular pattern was observed extending from the neovascular plexi on the graft side of the polypropylene mesh. At day 5, defined vessels with lobular ends occurred with high frequency. At day 7, the number of observed lobular structures was greatly reduced, and high frequencies of depressions in acrylic casts suggested protrusion of endothelial cell nuclei. By day 10, lobular structures were rare, well-defined microvascular plexi were contiguous with larger vessels, and depressions from endothelial cell nuclei appeared more shallow and less frequent. These findings suggest that (1) an immature lobular pattern representing either capillary outgrowth or extracapillary leakage occurs at day 3; (2) these immature lobules decrease, and more discrete capillaries increase by day 5; (3) vascular integrity is reestablished by day 7; (4) vascular plexi has regained full continuity, and there are suggestions that endothelial cell proliferation has subsided by day 10. **(WOUND REP REG 1995;3:213-20)**

---

Angiogenesis, the process by which blood vessels grow into a nonperfused space, is vital for the successful healing of all wounds and grafts. Angiogenesis involves the outgrowth of endothelial cells to form capillaries that revascularize injured tissues. Revascularization supplies oxygen and metabolites for collagen deposition and protein formation and re-

EC	Endothelial cell
ECM	Extracellular matrix
SEM	Scanning electron microscopy
TEM	Transmission electron microscopy

moves the waste products of metabolism. Knowledge of the pattern and kinetics of new blood vessel formation is important for the full understanding of wound healing because conditions which impair angiogenesis (e.g., advanced age and immunosuppression) also impair wound healing.

Numerous models have been used to study new capillary formation. Initial studies used the subcutaneous implantation of collagen and cellulose sponges to stimulate granulation tissue formation.<sup>1-6</sup> In that model, the sponge (porous foreign body) creates a space that the body attempts to heal, and the development

*From the Shriners Burns Institute and Department of Surgery, University of Cincinnati, Cincinnati, Ohio. Reprint requests: David G. Greenhalgh, MD, Shriners Burns Institute, 3229 Burnet Ave., Cincinnati, OH 45229.*

*Presented at the Fourth Annual Meeting of The Wound Healing Society, San Francisco, California, May 18-20, 1994.*

*Copyright © 1995 by The Wound Healing Society. 1067-1927/95 \$3.00 + 0 36/1/65314*

of granulation tissue within the implant is similar to that in a surgical wound. The rabbit cornea is the most widely accepted *in vivo* model for studying capillary formation.<sup>7,8</sup> That model has been used extensively to study the kinetics and patterns of angiogenesis induced by a variety of growth factors, tumors, and tissue injury.<sup>7-10</sup> Limitations of the rabbit cornea model are that it is inherently avascular and that inhibitors of angiogenesis exist in the cornea.<sup>7,8,11</sup> Because the commercial availability of infusible acrylic polymers, scanning electron microscopy (SEM) has been used to study patterns of corrosion casts of vascularization in normal and pathologic tissue. Corrosion casts are produced by filling an internal luminal system or space with a liquid medium which becomes solid *in situ*.<sup>12,13</sup>

This report describes a model which was adapted to directly evaluate the pattern of new vessel formation in full-thickness skin grafts. In this study, angiogenesis of full-thickness skin grafts on rats was evaluated by SEM and transmission electron microscopy (TEM) with the use of an infused acrylic polymer at serial time points after grafting. Ultrastructural morphologic characteristics of nascent vascular plexi developing during healing of skin grafts was evaluated. With these techniques, changes in subcellular structures of vascular plexi were observed in skin grafts during healing.

## MATERIALS AND METHODS

### Animals

All animal use was approved by the Institutional Animal Care and Use Committee (IACUC) at the University of Cincinnati and performed at the Shriners Burns Institute, Cincinnati Unit. Adult male Lewis rats (200 to 250 gm) were housed one per cage with a 12-hour light/dark cycle. Water and standard rodent chow was supplied *ad libitum*. Rats were anesthetized with an intraperitoneal injection of pentobarbital (0.1 mg/kg), and both hind limbs were shaved and swabbed with betadine and 70% ethanol. Temperature was maintained by performing the surgical procedure with the rats resting on a heating pad at a low setting. Full-thickness wounds (2 × 2 cm) were prepared by excising skin to the fascia on the proximal hind limbs. A polypropylene monofilament mesh (N-Terface; Winfield Laboratories, Inc., Richardson, Tex.) was placed on the wound base to identify the wound bed/graft boundary in later casting studies, and the autologous graft was secured with 2-0 silk sutures in its original orientation with a gauze bolster dressing.

### Cast preparation

At days 3, 5, 7, and 10, vascular casts of the grafts were prepared by means of a technique modified from Burger et al.<sup>7,8</sup> Each animal was anesthetized with intraperitoneal pentobarbital (0.15 gm/kg), and the descending thoracic aorta and suprahepatic vena cava were isolated. The descending thoracic aorta was cannulated with a 20-gauge polyethylene intravenous catheter, and a 1 ml volume of heparin flush solution was injected. After 1 minute, the animal was exsanguinated by thoroughly rinsing the descending thoracic aorta with warm (37° C) 0.9% normal saline solution after incising the vena cava. A total of 180 ml of flush solution was given with the final 60 ml of perfusate being clear. The suprahepatic vena cava was clamped, and the vasculature was filled with an acrylic polymer containing 2 gm benzoyl peroxide (Mercox; Ladd Research Industries, Inc., Burlington, Vt.) with moderate manual pressure. After 1 hour, the acrylic polymer had polymerized, and the grafts were excised through the skeletal muscle, and placed in normal saline solution overnight at 37° C. Mercox polymer is a favorable casting medium because it is nontoxic, has low enough viscosity to infiltrate the smallest capillaries, polymerizes rapidly, undergoes minimal shrinkage with curing, is resistant to corrosion by inorganic alkali, and is electron conductive but resistant to electron bombardment.<sup>12</sup>

### Preparation of samples for microscopy

Tissue for all light and TEM analysis was fixed with 2% glutaraldehyde (Ted Pella, Inc., Redding, Calif.)/2% paraformaldehyde (Electron Microscopy Sciences, Fort Washington, Pa.) in sodium cacodylate (0.1 mol/L, pH 7.4; Electron Microscopy). Samples for light and TEM were washed in sodium cacodylate (0.1 mol/L, pH 7.4) and postfixed in 1% osmium tetroxide in the same buffer. The tissue was washed, dehydrated in acetone, and embedded in an epon-araldite resin (Ted Pella).

Polymerized blocks were sectioned with a Reichart-Jung Ultracut E ultramicrotome (Leica Inc., Deerfield, Ill.). Light microscopy was performed to select areas for examination by TEM. For light microscopy, semithin sections (approximately 1 μm) were prepared and mounted on chrom-alum gelatin-coated slides. Sections were stained with toluidine blue and examined on a Nikon Microphot-FXA microscope (Nikon Inc., Melville, N.Y.). Thin sections for TEM were mounted onto 300 mesh copper grids, counterstained with uranyl acetate and lead citrate (Ted Pella), and examined with a JEOL JEM-100

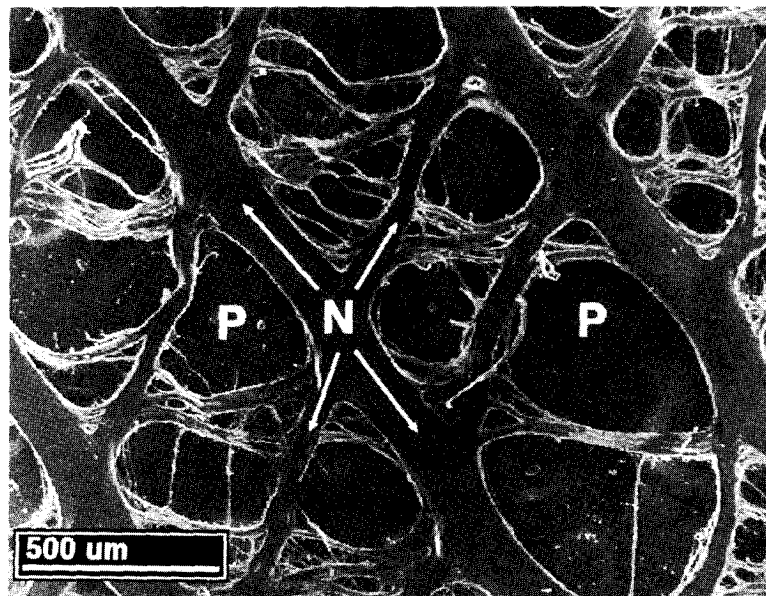


**Figure 1** Scanning electron micrograph of N-Terface polypropylene mesh dressing implanted beneath full-thickness skin grafts. The mesh (N) has a smooth, acellular structure with strands of material extending across the pores (P).

**Table 1.** Morphologic properties of casts infused with an acrylic polymer during healing of full-thickness skin grafts

Day	Lobules	Intact plexus	Endothelial cell nuclei	
			Frequency	Height
3	Many large	No	Low	Deep
5	Many small	Partial	High	Deep
7	Few small	Yes	High	Deep
10	Rare	Yes	High	Shallow

CXII transmission electron microscope (JOEL USA Inc., Peabody, Mass.).

Tissue for SEM was digested away from the acrylic polymer and polypropylene mesh at 37° C in 40% potassium hydrochloride for 6 hours, with three subsequent washes in normal saline solution, resulting in cast replicas of the blood vessels and the implanted polypropylene mesh. The digestion procedure was performed in stainless steel tissue baskets while maintaining the original orientation of the specimen (graft side up). The cast replicas were then washed in sodium cacodylate buffer 0.1 mol/L, postfixed in 1% osmium tetroxide (Electron Microscopy), and dehydrated with absolute ethanol. Samples were critical point-dried in a critical point drier (Denton DCP-1; Denton Vacuum Inc., Cherry Hill, N.J.), mounted on aluminum stubs, and sputter coated with gold-palladium.

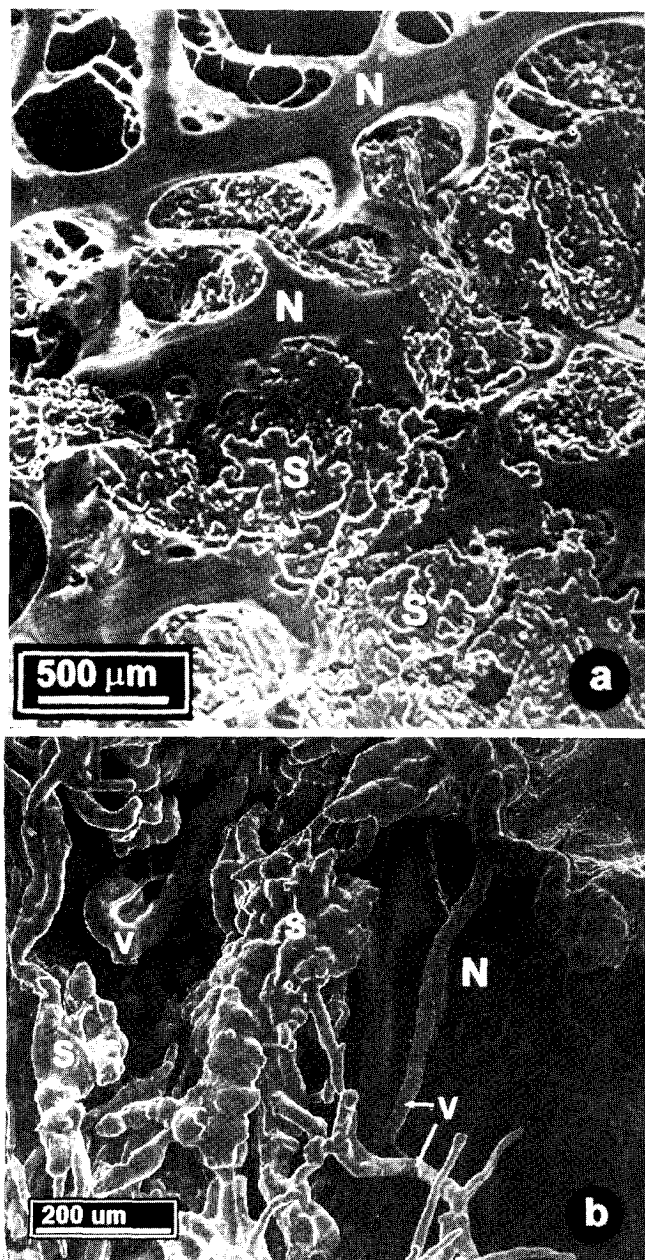
SEM was performed with a JEOL JSM-35 microscope, and images were recorded onto Polaroid type 52 sheet film or a Semicaps 1000 Digital Image Acquisition system (Semicaps Inc., Santa Clara, Calif.).

## RESULTS

All the animals survived the grafting procedure and gained weight until they were killed. Samples for microscopy were prepared from successful graft specimens as determined by an intact pink graft site. Thirty-six percent of the grafts did not succeed, which resulted from the rats dislodging specific grafts.

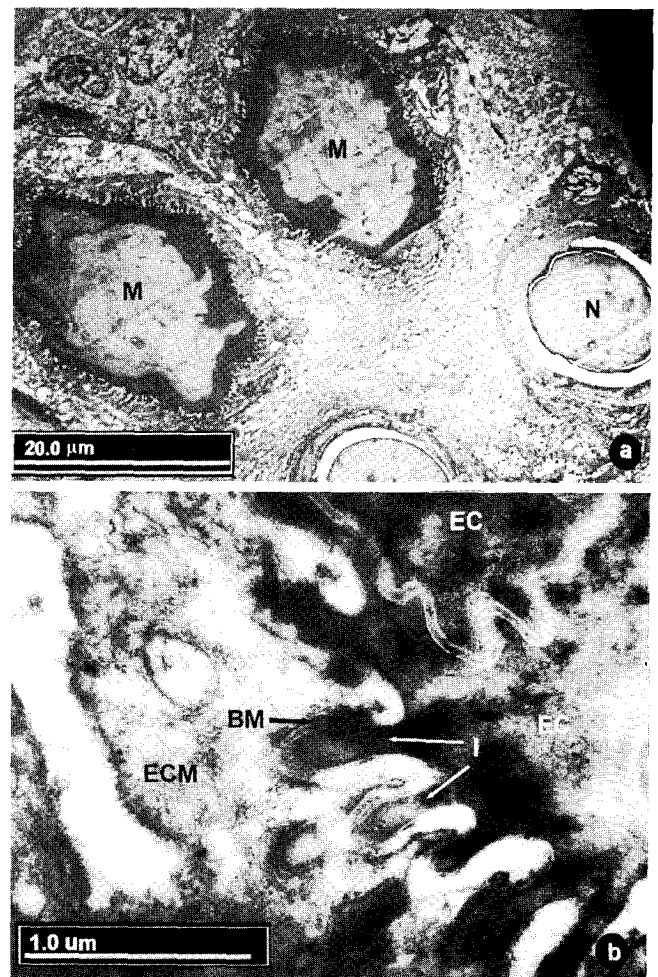
In the SEM, the polypropylene mesh is observed as irregularly spaced pores with a smooth "lattice-like" structure (Figure 1). The surface of the mesh has no cellular morphologic or nuclear depressions. Casts are examined with reference to the polypropylene mesh. Casts which are superior to the mesh represent vessels in the graft, whereas those that are inferior represent vessels in the wound.

By TEM, polypropylene mesh is observed as groups of three electron lucent profiles without surrounding endothelium or plasma membranes, and with an adjacent fibrous reaction (Figure 3, A). Vessels with the acrylic polymer have circumferential intact endothelial lumens filled with a noncellular, heterogeneous polymer.



**Figure 2** Scanning electron micrograph 3 days after application of full-thickness skin grafts. **A**, An immature lobular pattern of the vessel casts (S) extends from the wound bed through the polypropylene mesh (N). **B**, At a higher magnification, these immature lobules (S) are contiguous with casts of intact vessels (v), which are more linear and cylindrical. The polypropylene mesh (N) identifies the location of these vascular casts with the skin grafts.

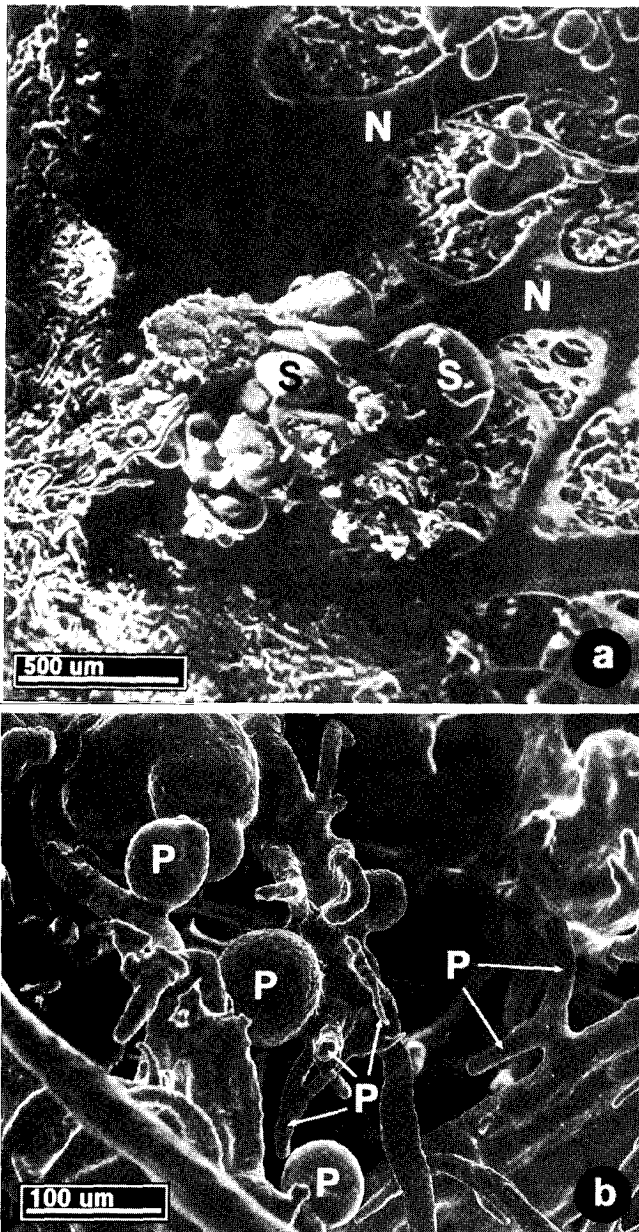
For both SEM and TEM, the entire graft is systematically examined in four separate grafts at each time point, and representative photomicrographs are taken. Concluding impressions with regard to frequency and pattern are determined after visualizing all fields of each graft and comparing them with the other grafts and time points.



**Figure 3** Transmission electron micrograph of wounds infused with an acrylic polymer 3 days after surgery. **A**, Two vessels filled with the acrylic polymer (M) are seen in proximity to the polypropylene mesh (N). There appears to be no extravasation of the polymer. **B**, Numerous interdigitations (I) form between ECs and ECM. Basement membrane (BM) joins the ECs with the ECM.

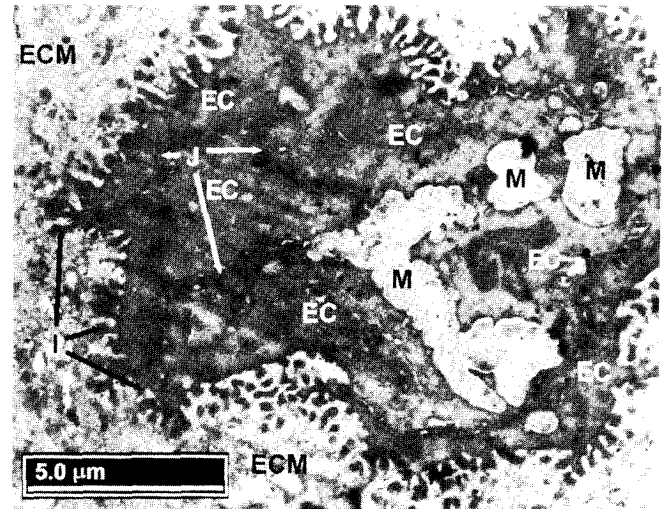
### Day 3

Table 1 contains a summary of the SEM observations. Three days after grafting was the earliest time point in which vascular corrosion casts could be constructed because of the fragility of any casts at earlier time points. Presumably, this condition was due to too few capillary casts beyond the polypropylene mesh boundary. At this early stage on SEM, an immature lobular pattern extended from the wound bed through the polypropylene mesh suggesting capillary ingrowth (Figure 2, A). The use of the polypropylene mesh identified the location of these vascular casts with the skin grafts. On closer inspection, at a higher magnification, these immature lobules were contiguous with casts of intact vessels, which were more linear and cylindrical (Figure 2, B). These immature lobules may represent distension of nascent vessels.



**Figure 4** Scanning electron micrograph 5 days after application of full-thickness skin grafts. **A**, Immature lobules (S) emerge through the polypropylene mesh (N). **B**, At higher magnification, spherical and cylindrical vascular projections (P) are contiguous with a more extensive vascular plexus.

TEM clearly showed the vessels filled with the acrylic polymer in proximity to the polypropylene mesh (Figure 3, A). Vessels containing the polymer had intact lumens consisting of continuous endothelial cell layers. At a higher magnification, the intact endothelial cells (EC) had numerous interdigitations forming into the extracellular matrix (ECM). A basement membrane could be seen joining the ECs with the extracellular matrix (ECM) (Figure 3, B). No extravasation of the acrylic polymer from the vessels could be seen. If



**Figure 5** Transmission electron micrograph of 5 days after application of full-thickness skin grafts. EC combine to form nascent vascular lumens which are filled with the acrylic polymer (M). In these newly forming vessels, numerous interdigitations (I) join ECs to ECM. Cell junctions (J) attach ECs together.

the polymer extravasates, it forms a pattern of needle-shaped crystals as seen with SEM. At all of the time points evaluated, no large vessels were visualized crossing the polypropylene mesh. This finding suggests that no signs of direct capillary connection (inosculation) into the graft occurred.

#### Day 5

The immature lobules at day 5 were still present but decreased in frequency when visually compared with the entire grafts from the previous time points (Figure 4, A). Spherical and cylindrical vascular projections were contiguous with a more extensive vascular plexus at a higher magnification (Figure 4, B). Larger buds were observed extending from existing vessels suggesting capillary formation. TEM shows an area of new capillary formation in which ECs were combining to form nascent vascular lumens which were filled with the acrylic polymer (Figure 5). The cell junctions were clearly seen to attach each EC together and to be in full continuity. Again, numerous interdigitations were seen joining the ECs to the ECM.

#### Day 7

By day 7, the immature lobular pattern was no longer seen (Figure 6). Capillary sprouts observed at earlier times were longer with more extensions. The sprouts could be seen to make "corkscrew" and "hairpin" turns. Numerous depressions were seen in these sprouts representing endothelial cell nuclei (Figure 6, B), which were consistent with previously published reports.<sup>11</sup> The EC nuclei are located in the cell such that they project

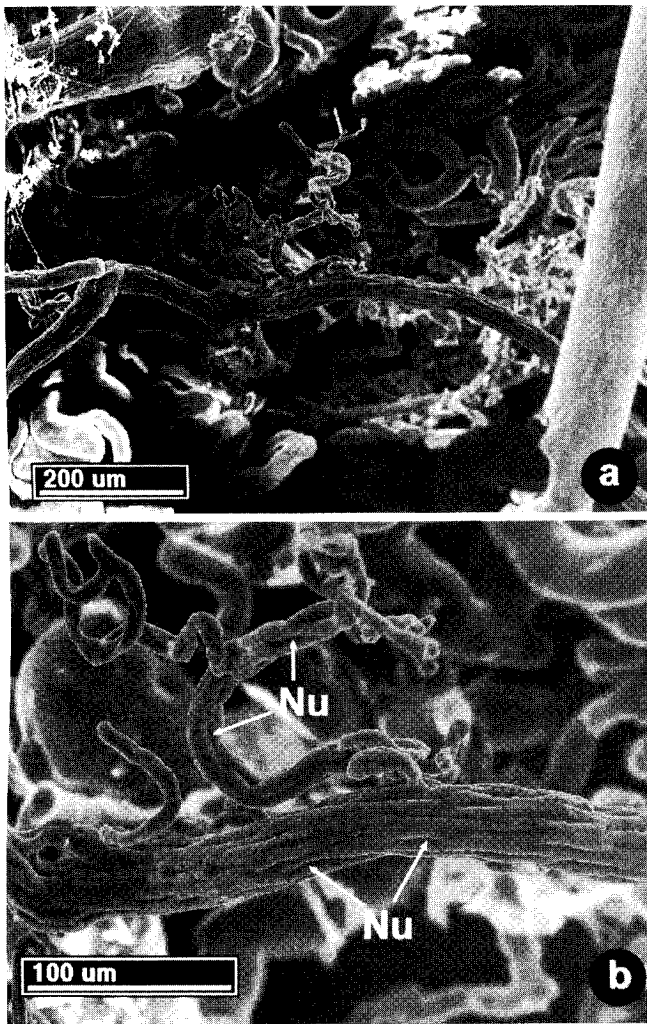


**Figure 6** Scanning electron micrograph 7 days after application of full-thickness skin grafts. **A**, Immature lobules are not found in the vascular casts. Vessels form more complete networks. **B**, At higher magnification, numerous depressions in vascular casts identify EC nuclei (*Nu*). Branching vessels are also observed with high frequency.

into the lumen of the vessel.<sup>14</sup> This luminal projection would therefore create a depression in a casted vessel on SEM as seen in Figure 6, *B*. Vascular continuity appeared to be reestablished at this time point.

#### Day 10

By day 10, the vascular plexi had regained full continuity. Depressions from endothelial cell nuclei seen on the cast replicas of the vessels were less pronounced by this time. These new vessels had elongated and formed vascular loops (Figure 7).

### DISCUSSION

Similar to other forms of healing, engraftment of skin involves three phases:

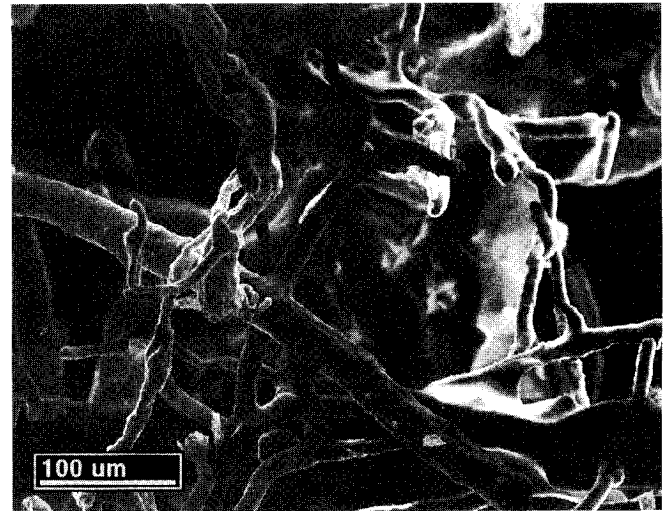


**Figure 7** Scanning electron micrograph 10 days after application of full-thickness skin grafts. Cast replicas show a highly reticulated vascular plexus. Depressions in casts from EC nuclei are less prominent and less frequent.

1. **Imbibition.** Imbibition begins immediately after placement of the graft. Nutrients are supplied by means of diffusion from the graft bed, and the graft is held in place by weak fibrin and fibronectin bonds.
2. **Revascularization.** Revascularization begins at 24 to 48 hours and is complete by 4 to 6 days. This process has been explained by two possible mechanisms: inosculation, previously formed capillaries connecting directly with those remaining in the graft; and neovascularization, the migration of endothelial cells from a venule into an avascular space, creation of a new lumen, and reanastomosis with arterioles. In skin grafts, endothelial cells migrate into the graft to form new capillaries in a process similar to angiogenesis in other wounds.
3. **Organization.** Organization begins at 4 days as fibroblasts migrate into the graft. These cells synthesize and deposit collagen along the fibrin scaffolding to increase the resistance of the graft to shearing.<sup>15</sup>

In this study, revascularization of the graft followed normal patterns and timing of wound healing. Capillary buds and lobules were seen by day 3. During the following days, new vessels formed with increased vascular networks. At day 5 lobules decreased, and by day 7 vascular integrity appeared to be reestablished. There were numerous EC nuclei depressions at day 7, which decreased by day 10.

The observations of the acrylic polymer infiltration are consistent with the known phases of wound healing and graft revascularization.<sup>11,15</sup> In subcutane-

ous sponge models, an intense inflammatory infiltrate began at 6 hours and peaked by 48 to 72 hours.<sup>1,16</sup> Subsequently, there was a rapid decline in white cells between 4 and 8 days after implantation as collagen organization occurred.<sup>5,17</sup> In the model presented here, early inflammatory time points were not studied because vascular corrosion casts could not be obtained before 3 days in this graft revascularization model. The graft is initially attached to the wound bed by weak fibrin and fibronectin bonds, and thus no vascular casts would be obtained until preliminary revascularization of the graft bed had occurred.

With SEM, immature lobular patterns of vascular corrosion casts were seen by day 3. These images may represent either newly formed vessel buds or artifact caused by the acrylic polymer extravasating through the immature vessels. TEM specimens from the same time point, however, showed vessels filled with the polymer with intact lumens and continuity of the endothelial cell layer near the polypropylene mesh. Therefore, TEM images suggest that the immature lobules seen by SEM represent intact vessels. Formation of these immature lobules may result in part from distension of vessels during the infusion of the acrylic polymer or a true anatomic phenomenon.

TEM images at all time points showed a unique characteristic of the vessels. The matrix side of the vessels consisted of numerous interdigitations, whereas the luminal surface was much more smooth. These projections greatly enhance the surface area of these vessels in contact with the surrounding ECM. This increased surface area possibly plays a role in facilitating angiogenesis by promoting the mobility of the individual ECs toward an increasing gradient of an angiogenic factor.

Direct angiogenesis results from angiogenic factors acting directly on ECs causing new capillary formation, whereas indirect angiogenesis occurs by the actions of growth factors that recruit inflammatory cells which release factors that lead to direct angiogenesis.<sup>11,18,19</sup> Numerous compounds have been studied and reported to have angiogenic activity. Basic fibroblast growth factor, acidic fibroblast growth factor, transforming growth factor beta, transforming growth factor alpha, epidermal growth factor, tumor necrosis factor alpha, prostaglandin of the E series, platelet-derived growth factor, platelet-derived EC growth factor, EC-stimulating angiogenesis factor, vascular permeability factor, and angiogenin have all been reported as angiogenic.<sup>20-29</sup> In previous studies, vascular bed formation (believed to be direct angiogenesis) could be seen between 27 and 48 hours,

depending on the model used. Chemical cautery of the cornea is a model of indirect angiogenesis, which elicits a high degree of inflammation leading to early capillary bud formation.<sup>7,8</sup> Early capillary bud formation can also be seen in the model using implantation of tumor fragments in the cornea, an example of direct angiogenesis.<sup>9</sup> In the sponge model of Phillips, Whitehead, and Knighton<sup>11</sup> (indirect angiogenesis), buds were seen slightly later (48 hours) because of a more moderate degree of inflammation when compared with the corneal cautery model. In this study, it is presumed that both direct and indirect angiogenesis occur. Cut blood vessels release angiogenic factors which cause new capillary formation by direct angiogenesis. The process of engraftment also results in inflammation, with indirect angiogenesis aiding in new capillary formation. Many studies have been performed to evaluate the aforementioned growth factors with respect to their angiogenic activity with *in vivo* and *in vitro* models.<sup>21-29</sup>

Results of this study show that the acrylic polymer can be used to prepare vascular corrosion casts in dermal grafts to study neoangiogenesis. A polypropylene mesh, which is a nonadherent dressing used in the clinical setting, can be used to define the boundary and orientation of the dermal graft/wound bed interface by allowing vessel growth to occur through its pores. Early in revascularization, a yet unexplained lobular pattern exists in the invading vessels. Associated with this finding is a convoluted pattern of the matrix side of the vessels presumably aiding in the process of angiogenesis. Over time, capillaries invading the graft increase in frequency, and by day 7 revascularization is reestablished. Of all the samples evaluated, none showed any signs of direct capillary connection (inosculation) to the graft.

Ultrastructural findings of this study are consistent with the clinical behavior of skin grafts. By day 3, blanching can be observed in the skin graft corresponding to the earliest time that vessels are obtained in the polypropylene mesh. The graft stabilizes as the vascular network regains full continuity between days 5 to 10 after application. These results provide additional evidence to identify the cellular mechanisms by which skin grafts become vascularized. In this rat model, revascularization of the skin graft appears to proceed in a similar temporal sequence as occurs in human skin grafts. Examination by electron microscopy of vascular corrosion casts and infused acrylic polymer provides an index for assessment of reperfusion during healing of skin wounds with native or experimental skin grafts.

**ACKNOWLEDGMENTS**

Supported by Shriners of North America with grant Nos. 15846 and 15862. The authors thank North Lilly for the excellent technical support in preparing the electron micrographs.

**REFERENCES**

1. Viljanto J, Kulonen E. Correlation of tensile strength and chemical composition in experimental granuloma. *Acta Path Microbiol Scand* 1962;56:120-6.
2. Viljanto J. Cellstic. A device for wound healing studies in man: description of the method. *J Surg Res* 1976;20:115-9.
3. Nemlander A, Ahonen J, Wiktorowicz K, von Willebrand E, Hekali R, Lalla M, Hayry P. Effect of cyclosporine on wound healing. *Transplantation* 1983;36:1-6.
4. Woessner JF, Boucek RJ. Connective tissue development in subcutaneously implanted polyvinyl sponge. *Arch Biochem Biophys* 1961;93:85-94.
5. Mahadevan V, Hart IR, Lewis GP. Factors influencing blood supply in wound granuloma quantitated by a new in vivo technique. *Cancer Res* 1989;49:415-9.
6. Lindenbaum ES, Kaufman T, Beach D, Maroudas NG. Uterine angiogenic factor induces vascularization of collagen sponges in guinea-pigs. *Burns* 1989;15:225-9.
7. Burger PC, Chandler DB, Klintworth GK. Corneal neovascularization as studied by scanning electron microscopy of vascular casts. *Lab Invest* 1983;48:169-80.
8. Burger PC, Chandler DB, Klintworth GK. Scanning electron microscopy of vascular casts. *J Electron Microsc Tech* 1984;1:341-8.
9. Ausprunk DH, Folkman J. Migration and proliferation of endothelial cells in preformed and newly formed blood vessels during tumor angiogenesis. *Microvasc Res* 1977;14:53-65.
10. Gimbrone MA, Cotran RS, Leapman SB, Folkman J. Tumor growth and neovascularization: an experimental model using the rabbit cornea. *J Natl Cancer Inst* 1974;52:413-9.
11. Phillips GD, Whitehead RA, Knighton DR. Initiation and pattern of angiogenesis in wound healing in the rat. *Am J Anat* 1991;192:257-62.
12. Lametschwandtner A, Lametschwandtner U, Weiser T. Scanning electron microscopy of vascular corrosion casts: techniques and applications: updated review. *Scan Microsc* 1990;4:889-941.
13. Hodde KC, Steeber DA, Albrecht RM. Advances in corrosion casting methods. *Scan Microscopy* 1990;4:693-704.
14. Ross MH. Lymphatic system. In: Ross MH, Rotorell LJ, editors. *Histology: a text and atlas*. Baltimore: Williams & Wilkins, 1989:342-3.
15. Greenhalgh DG, Staley MJ. Burn wound healing. In: Richard RL, Staley MJ, editors. *Burn care and rehabilitation: principles and practice*. Philadelphia: F.A. Davis, 1994:70-102.
16. Lamont PM. Mechanisms of wound healing. *Prob Gen Surg* 1989;6:183-93.
17. Boucek RJ, Noble NJ. Connective tissue: a technique for its isolation and study. *Arch Pathol* 1955;59:553-8.
18. Polverini PJ, Cotran RS, Gimbrone MA, Unanue E. Activated macrophages induce vascular proliferation. *Nature* 1977;269:804-6.
19. Knighton DR, Hunt TK, Scheuenstuhl H, Halliday BJ, Werb Z, Banda MJ. Oxygen tension regulates the expression of angiogenesis factors by macrophages. *Science* 1983;221:1283-5.
20. Phillips GD, Fiegel VD, Knighton DR. Putative angiogenesis factors: a review. *Wounds* 1992;4:94-107.
21. Fett JW, Strydom DJ, Lobb RR, Alderman EM, Bethune JL, Riordan JF, Valle BL. Isolation and characterization of angiogenin, an angiogenic protein from human carcinoma cells. *Biochemistry* 1985;24:5480-6.
22. Knighton DR, Phillips GD, Fiegel VD. Wound healing angiogenesis: indirect stimulation by basic fibroblast growth factor. *J Trauma* 1990;30:S134-44.
23. Lobb RR, Alderman EM, Fett JW. Induction of angiogenesis by bovine brain derived class I heparin-binding growth factor. *Biochemistry* 1985;24:4969-73.
24. Schreiber A, Winkler ME, Derynck R. Transforming growth factor-alpha: a more potent angiogenic mediator than epidermal growth factor. *Science* 1986;232:1250-3.
25. Leibovich SJ, Polverini PJ, Shepard HM, Wiseman DM, Shively V, Nuseir N. Macrophage-induced angiogenesis is mediated by tumor necrosis- $\alpha$ . *Nature* 1987;329:630-2.
26. Connolly DT, Heuvelman DM, Nelson R, Olander JV, Eppley BL, Delfino JJ, Siegel NR, Liemgruber RM, Feder J. Tumor vascular permeability factor stimulates endothelial cell growth and angiogenesis. *J Clin Invest* 1989;84:1470-8.
27. Ishikawa F, Miyazono K, Hellman U, Drexler H, Wernstedt C, Hagiwara K, Usuki K, Takaku F, Risau W, Heldin CH. Identification of angiogenic activity and the cloning and expression of platelet-derived endothelial cell growth. *Nature* 1989;338:557-62.
28. Taylor CM, Kissun RD, Schor AM, McLeod D, Garner A, Weiss JB. Endothelial cell-stimulating factor in vitreous from extraretinal neovascularizations. *Invest Ophthalmol Vis Sci* 1989;30:2174-8.
29. BenEzra D. Neovasclogenetic ability of prostaglandins, growth factors, and synthetic chemoattractants. *Am J Ophthalmol* 1978;86:455-61.

Availability of JOURNAL Back Issues

As a service to our subscribers, copies of back issues of WOUND REPAIR AND REGENERATION are maintained and are available for purchase from the publisher, Mosby-Year Book, Inc., at a cost of \$15.00 per issue. The following quantity discounts are available: 25% off on quantities of 12 to 23, and one third off on quantities of 24 or more. Please write to Mosby-Year Book, Inc., Subscription Services, 11830 Westline Industrial Dr., St. Louis, MO 63146-3318, or call (800) 453-4351 or (314) 453-4351 for information on availability of particular issues. If unavailable from the publisher, photocopies of complete issues are available from University Microfilms International, 300 N. Zeeb Rd., Ann Arbor, MI 48106; 313 761-4700.